Journal of The Electrochemical Society, **154** (12) E187-E193 (2007)
0013-4651/2007/154(12)/E187/7/$20.00 © The Electrochemical Society

Electrodeposition of Metal Iron from Dissolved Species in Alkaline Media

A. Allanore,[a,*,z] H. Lavelaine,[a] G. Valentin,[b] J. P. Birat,[a] and F. Lapicque[b]

[a]*Arcelor Research SA, Voie Romaine, F-57283 Maizières les Metz, France*
[b]*Laboratoire des Sciences du Génie Chimique, CNRS-ENSIC-INPL, F-54001 Nancy, France*

The electrodeposition of metal iron from iron dissolved species in alkaline media has been investigated. Dissolved ferric species in equilibrium with hematite (α-Fe_2O_3) have been electrochemically identified and their reduction to iron was demonstrated. The reduction efficiency was poor, however, because of the low concentration of dissolved matter (2.6×10^{-3} M). In order to determine more precisely the electrochemical features of the deposition reaction from iron ions, more concentrated solutions at 1.9×10^{-2} M have been obtained using an iron anode as the ion source. Voltammetric and chronoamperometric investigations using a rotating disk electrode revealed that such concentrated solutions contain ferric and ferrous species, with higher concentration of the trivalent form. Metal can be deposited with higher current efficiency in these concentrated solutions with less than 30% of the current spent in hydrogen evolution.
 [DOI: 10.1149/1.2790285]

Manuscript submitted June 13, 2007; revised manuscript received August 30, 2007. Available electronically October 16, 2007.

Within the European project "Ultralow CO_2 in Steelmaking (ULCOS)" one of the possible routes investigated for iron production with a potential for a breakthrough reduction of greenhouse gas emissions involves electrochemical techniques. The winning of iron from its ore by electrolysis in alkaline media can be considered as a possible promising process as shown early by Lloyd[1] and later by Leduc et al.[2] The range of working temperatures allowed by an aqueous-based liquid is an asset of this route. Furthermore, alkaline water electrolysis is considered a mature technology so that challenges related to materials such as reliable anodes for the oxygen evolution reaction[3] have already been overcome. Whereas the production of iron powder in an acidic medium has been studied for decades by the metal industries,[4,5] the deposition of iron in a basic medium has been less studied. The alkaline conditions considered here are 50 wt % sodium hydroxide solutions at 110°C, as already determined as suitable for iron oxide electrolysis.[6] For the process under study, the main overall reaction at the cathode is the reduction of hematite

$$Fe_2O_3 + 3H_2O + 6e^- \rightarrow 2Fe + 6\ OH^- \quad [1]$$

The oxygen evolution reaction occurs at the anode

$$4\ OH^- \rightarrow O_2 + 2H_2O + 4e^- \quad [2]$$

The reaction of interest at the cathode is conducted in a two-phase medium where suspended particles of iron oxide are reduced in the immediate vicinity of the electrode, in a so-called "solid-state" process.[6] Such a single-step transfer of six electrons to the particle concurrently with oxygen removal from the bulk of the oxide solid phase at 100°C is questionable. A more precise description of iron chemistry in alkaline media is therefore required, because a conventional approach in electrochemistry would suggest that metallic iron is formed from iron oxide by electrochemical reactions when iron ionic species are reduced at the electrode.

Thermodynamics provides the first elements to start the discussion. Most papers dealing with iron oxide(III) in alkaline media mention its poor dissolution at around 2×10^{-3} M in 18 M NaOH at 100°C [6] into ferric species, mainly in the form $Fe(OH)_4^-$.[7] The corresponding reaction is

$$Fe_2O_3 + 3H_2O + 2\ OH^- \rightleftharpoons 2Fe(OH)_4^- \quad [3]$$

Electrochemical reduction of the iron hydroxyl anion leads to ferrous species through Reaction 4, with $Fe(OH)_3^-$ as the predominant form of Fe(II) in such alkaline media[8]

$$Fe(OH)_4^- + e^- = Fe(OH)_3^- + OH^- \quad [4]$$

The equilibrium potential for Reaction 4 depends on the compared activities of ferric and ferrous ions. The reduction of the ferrous anion can lead to formation of metal iron

$$Fe(OH)_3^- + 2e^- = Fe + 3\ OH^- \quad [5]$$

This reaction competes with the hydrogen evolution reaction

$$2H_2O + 2e^- \rightleftharpoons H_2 + 2\ OH^- \quad [6]$$

For the deposition reaction (Eq. 5), the Fe(II) ion activity determines the equilibrium potential through the Nernst equation. The standard equilibrium potentials for these electrochemical reactions can be calculated from published thermodynamics data.[8] The nonideal behavior of such concentrated electrolyte can be taken into account for H_2O and OH^- species from activities compiled by Balej.[9] Experimental activity coefficients for $Fe(OH)_x^{y-}$ anions are not taken into account because of lack of available data. In 50 wt % NaOH – H_2O electrolyte at 110°C, and in the case of equal activity in dissolved iron species, the equilibrium potential for Reaction 4 is −870 mV/SHE. Considering ferrous hydroxyl ions with an activity of 10^{-4} M, the calculated potential for the deposition reaction (Reaction 5) is near −1300 mV/SHE, whereas increasing the activity to 2×10^{-2} M shifts the potential to −1215 mV/SHE. This value is close to the HER (Eq. 6) potential in these conditions (−1190 mV/SHE).

A second source of information about iron electrochemistry is provided by published investigations on iron corrosion in strongly alkaline media, where the anodic and cathodic reactions occurring at iron electrodes have been identified. An electrochemical signal due to the reduction of oxidized iron to metal was observed by Andersson and Ojefors[10] in 4.5 M KOH and attributed to the reaction of ferrous hydroxide $Fe(OH)_2$. This process is the only solid-state reaction that can lead to the formation of metal but cannot occur in the alkaline process under study because $Fe(OH)_2$ is known to disproportionate at temperature greater than 60°C, as shown by Le and Ghali.[11] Armstrong and Baurhoo[12] investigated the electrochemistry of dissolved Fe(II) and Fe(III) species ions at temperatures up to 80°C and demonstrated the existence of Reaction 4 by ring disk studies. They also detected iron deposition (Reaction 5) but did not study this reaction any further.

A third aspect of iron electrochemistry in alkaline media is related to the formation of ferrate, the +VI iron species FeO_4^{2-},[13,14] which is produced at +600 mV/SHE in 50 wt % NaOH from dissolution of iron anodes. Bouzek et al.[14] investigated the electrochemical generation of ferrates and observed a current recorded below −1090 mV/SHE; this current was attributed to the Fe(II) reduction (Reaction 5), although without any clear-cut evidence.

* Electrochemical Society Student Member.
z E-mail: antoine.allanore@arcelormittal.com

The literature survey together with the elements of thermodynamics presented here reveal that ion species can exist in the presence of iron oxides in highly alkaline media at 110°C. This paper aims at specifying and quantifying the reactions of iron-dissolved species (III) and (II) in alkaline media leading to deposition of metal. To evaluate the possible role of dissolved species in the Reaction 1 pathway, a first series of experiments was conducted to quantify the deposition reaction from a solution saturated with hematite, where the iron oxide particles are kept away from the cathode. Then, a more precise description of the deposition reaction from ionic species was obtained by using a more concentrated solution of iron species, prepared by the anodic dissolution of an iron rod.

Experimental

The cell consisted of a polytetrafluoroethylene (PTFE) cylindrical beaker (400 cm^3 capacity) embedded in a stainless steel cell with a two-walled jacket. 330 cm^3 of liquid was introduced in the vessel for the experiments. Circulation of oil in the jacket made it possible to accurately control the temperature of the electrolyte solution. All the experiments were conducted at an electrolyte temperature of 110 °C, and a slight nitrogen bubbling was used to reduce the influence of oxygen on chemical and electrochemical processes. A PTFE round lid fixed on the cell cover allowed support of the electrodes. Two different anodes were used: the first was a 50 cm^2 platinum cylinder, while the second, used for investigating highly concentrated solutions of iron ions, was a 130 cm^2 iron sheet, 150 μm thick. A reference electrode Hg/HgO (KOH 10 M), equipped with a glass extension with a sintered junction filled with KOH 10 M, was used for measuring the potential of the two electrodes. The reference potential (E = 0.016 V/SHE at 110°C) was controlled before and after each experiment using a saturated calomel electrode in a 10 M KOH electrolyte at room temperature (E = 0.245 V/SHE); no deviation of the reference electrode potential was observed. All potentials given were converted to the standard hydrogen scale.

The rotating disk working electrode was made with a PTFE disk holder screwed on a rotating device Radiometer BM EDI-101. Disks of 1 cm^2 were machined out of pure graphite (EL + 50PT, Carbone Lorraine, France) and inserted in the PTFE holder. The potentiostat used was a Solartron 1286 controlled by a general purpose interface bus (GPIB) driven by a user-developed LABVIEW program for command of the electrochemical device together with data acquisition and treatment.

Sodium hydroxide solutions at 50 wt % (18 M) were prepared by dissolving NaOH flakes (Prolabo 97% purity, maximum 2.5% Na_2CO_3) in Milli-Q water (18.2 MΩ). The pH of the solutions at 25°C was about 15.

In the first experimental part, ferric species were produced from the dissolution of hematite oxide particles (average diameter = 7.5 μm, Prolabo 85% purity minimum) contained in a 6 cm^3 compartment. This chamber, installed at the bottom of the beaker, was in contact with the solution through a porous diaphragm (1 μm pores) separating the chamber and the rest of the cell. This diaphragm avoided the presence of hematite in the vicinity of the electrodes. Approximately 10 g (2 cm^3) of hematite powder were introduced into the chamber; this arrangement made it possible to reach saturation of the solution with ferric ions. After introducing the hematite, the electrolyte solution was poured in and the chamber covered by the filter holder. The hematite chamber was thereafter placed at the bottom of the cell and gravity allowed its mechanical stability in the electrolyte solution under study. The analysis of the solution revealed that saturation with ferric species, with a concentration at 2.46×10^{-3} M, was attained after 3 h at 110°C and the electrochemical tests were started thereafter. In the second part, experiments were conducted in a hematite-free solution. Iron ions were generated by dissolving an iron anode with an area 100 times larger than that of the graphite electrode. The same alkaline electrolyte as in the first section was used.

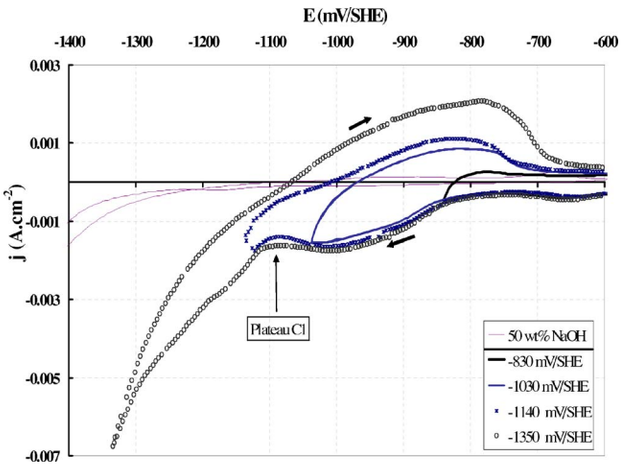

Figure 1. (Color online) Voltammograms recorded at 10 mV s^{-1} and 1000 rpm in a 2.64×10^{-3} M dissolved iron solution in equilibrium with hematite. Potentials given are the limits of the cathode scans, while the anodic potential limit was kept at −250 mV/SHE. 18 M NaOH medium at T = 110°C.

Scanning electron microscopy (SEM) images of deposits were made using a JEOL JSM-840 apparatus with a 15 kV beam. Faradaic yield for iron deposition was determined by measurement of the iron amount obtained on the disk. For this purpose, deposits were dissolved in 2 M HCl solution and corresponding iron-ion concentration was determined by inductively coupled plasma analysis using standard iron nitrate solutions (TechLab plasma emission standard) with the same acid concentration.

To determine the iron-ion concentrations in the NaOH electrolyte, the alkaline samples were acidified by adding HCl to bring the pH below 2. Blank alkaline solutions at the same concentrations were submitted to the same treatment for reference.

Results

Deposition of iron from a Fe(III) solution saturated with hematite.— The voltammetric curves recorded on a graphite electrode (1 cm^2) are presented in Fig. 1 for different potentials. Two scans were usually required to reach the steady-state behavior of the electrode. The graph suggests that several reactions are involved in the overall process, as mentioned in previous papers:

Iron (III)/iron (II) at plateau C1.— At −900 mV/SHE, reduction of ferric ions[12]

$$Fe(OH)_4^- + e^- = Fe(OH)_3^- + OH^- \quad [7]$$

At −750 mV/SHE, oxidation of ferrous ions can be considered following Reaction 4.

Iron (II)/Iron (0), more negative than plateau C1.— At −1150 mV/SHE, reduction of ferrous species[14]

$$Fe(OH)_3^- + 2e^- = Fe + 3\ OH^- \quad [8]$$

At −800 mV/SHE, oxidation of metal iron occurring through[15]

$$Fe + 2\ OH^- \rightarrow Fe(OH)_2 + 2e^- \quad [9]$$

which is the reverse reaction of Reaction 5 usually observed. As previously mentioned, neutral ferrous hydroxide is unstable above 110°C, and in the present operating conditions, it should be assigned to magnetite formation through the overall reaction

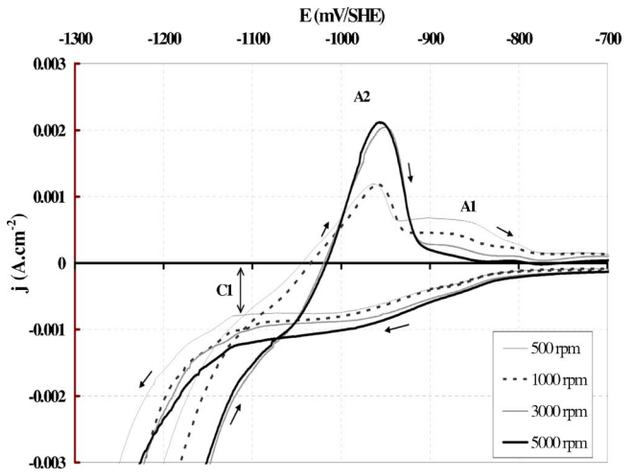

Figure 2. (Color online) Effect of the rotating speed on (*j-E*) curves recorded at 2 mV s^{-1} in the 2.64×10^{-3} M dissolved iron solution in equilibrium with hematite. 18 M NaOH medium at $T = 110°C$.

$$3Fe + 8\ OH^- \rightarrow Fe_3O_4 + 4H_2O + 8e^- \quad [10]$$

Iron deposition reaction (Reaction 5) cannot be clearly distinguished in voltammograms because the additional reduction of water into hydrogen, which occurs at approximately −1250 mV/SHE on graphite in Fe-free NaOH solutions, might occur at less negative potential because of the electrocatalytic properties of iron deposited with respect to carbon.[16]

The effect of the rotating speed of the electrode has been investigated at 2 mV/s and is presented in Fig. 2. The cathode wave appearing below −800 mV/SHE was slightly increased at higher rotation rates. The current variation was plotted in Fig. 3, using the conventional Koutecky–Levich relation. The diffusion-controlled contribution was found to be independent of the potential considered. The same approach was used for the most cathodic part of the signal (data not shown), where the value for the diffusion term was found to be dramatically affected by the potential: this is probably due to the occurrence of the two competing reactions, Reactions 5 and 6, and the Koutecky–Levich plot could not be used. Concerning the anodic signal, two peaks are observed at this low sweep rate: A2

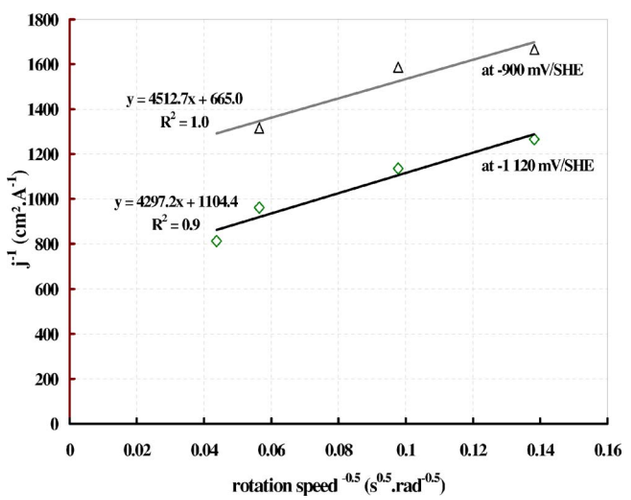

Figure 3. (Color online) Koutecky–Levich plots for the C1 plateau (current recorded on the forward scan) obtained from Fig. 2, in the 2.64×10^{-3} M dissolved iron solution in equilibrium with hematite. 18 M NaOH medium at $T = 110°C$.

Table I. Chronoamperometric investigation of deposition from the 2.64×10^{-3} M iron NaOH solution saturated with hematite. Rotation rate = 2500 rpm.

Imposed potential (mV/SHE)	Average current density (mA cm^2)	Faradaic yield ($3e^-$ based, %)
−1150	0.75	3
−1200	2.60	5
−1250	5.20	8
−1300	13.40	1.4
−1400	21.60	1.6

at −950 mV/SHE, which may be assigned to Reaction 10, and A1, which may be attributed to equilibrium (Reaction 4) at a high Fe(III)/Fe(II) ratio.

With the aim of evaluating the HER intensity, a chronoamperometric study of Fe deposition was conducted at constant rotation speed and various potentials. A freshly polished electrode was used for each potential value and at least 10 C/cm^2 of electrical charge were passed. At the end of each experiment, the cathode was directly immersed in an acidified solution to dissolve the deposited metal prior to inductively coupled plasma (ICP) analysis. Values for the average current density were calculated by dividing the electrical charge by the duration of the experiment and the electrode surface. As shown in Table I, the faradaic yield of the deposition conducted in the low-concentrated Fe solutions was usually low.

The surface of the deposit is shown in Fig. 4. Although not entirely covering the electrode surface, the metal deposited consists of fine and regular crystal aggregates, with a size of about 1 μm. The regular aspect of the deposit formed with a significant side hydrogen evolution is probably due to its moderate average thickness, around 0.2 μm for the example selected.

Deposition of iron from concentrated iron-ion solutions.— Dissolution of the iron electrode.— The electrochemical system used in this new experiment was the same as that used previously, except for the anode, which was an Fe foil, and the hematite-containing chamber, which was removed from the cell. Due to the 100 ratio of electrode areas, a very low current density was applied at the anode surface which was then weakly polarized. A platinum wire was immersed between the two electrodes to act as an Fe(III)/Fe(II) probe.

A first experiment was carried out without imposing a current between the two electrodes, while the potentials were continuously monitored. As shown in Fig. 5, the potentials remained fairly constant during the experiment, about −950 mV/SHE for the graphite rotating disk electrode and −1050 mV/SHE for the Fe electrode, respectively, and the net current was ca. 1 μA during the test. The platinum wire indicated an open-circuit potential of −750 mV/SHE, revealing the coexistence of Fe(III) and Fe(II) in the solution. The

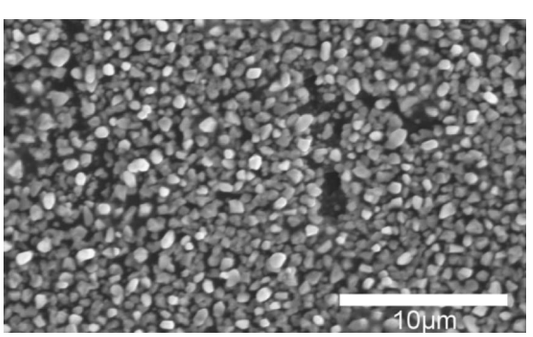

Figure 4. SEM image of Fe deposit obtained at −1250 mV/SHE on a graphite electrode from the 2.64×10^{-3} M iron species solution. Rotating speed = 2500 rpm. Approximate average thickness = 0.2 μm.

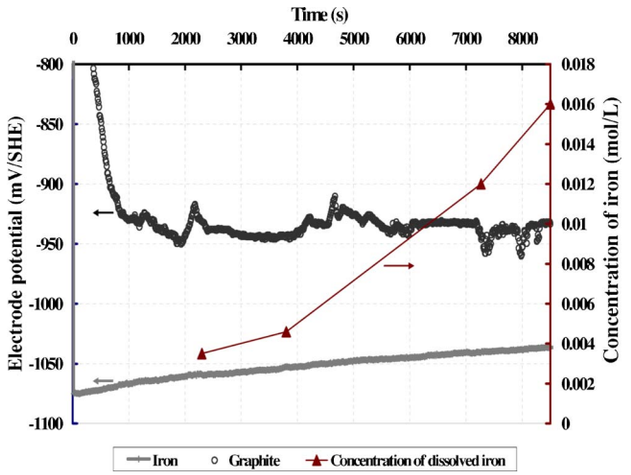

Figure 5. (Color online) Potentials of the graphite and iron electrodes, (o) and (+), respectively, and concentration in dissolved iron (dark triangles) during dissolution of the iron sheet without imposed current. Rotating speed = 3500 rpm.

final solution obtained has a light blue color which can be attributed to the Fe(II) hydroxyl ion according to Scholder[17] or Doisneau and Tremillon.[18]

ICP analysis showed the regular accumulation of dissolved iron in the cell (Fig. 5). The concentration obtained at the end of the test, about 0.016 M corresponding to 295 mg of iron, was consistent with the weight loss of the iron electrode, estimated at 210 mg. Such a figure is in agreement with iron dissolution experiments under similar conditions.[17]

Chronoamperometry with the same experimental device was conducted afterward at 0.1 A cm^{-2} on the cathode to promote dissolution of the iron anode. The variations of potential are presented in Fig. 6 together with the concentration of dissolved iron species. The anode potential was approximately constant at −1050 mV/SHE during the test. The cathode potential and the concentration of dissolved species increased with time simultaneously. The mass balance on iron was established, and the anode weight loss corresponded to 88% of the sum of the weight of deposited metal at the cathode and the accumulated dissolved iron in the cell. The color of

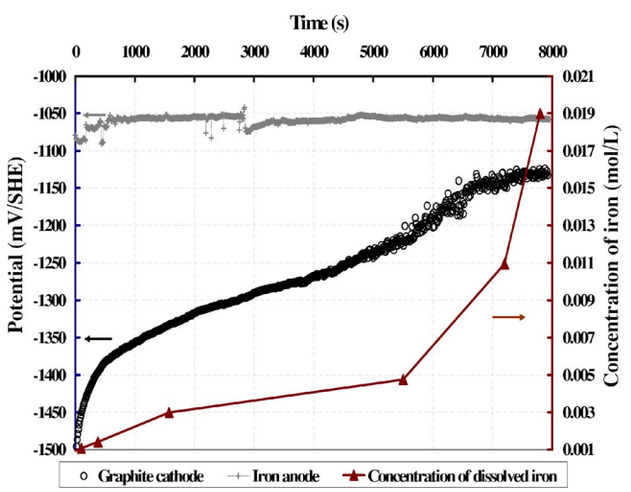

Figure 6. (Color online) Anode and cathode potentials (*o*) and (+), respectively, and concentration in dissolved iron (dark triangles) during dissolution of the anode at imposed current density (0.1 A cm^{-2}) on the cathode. Rotating speed = 3500 rpm.

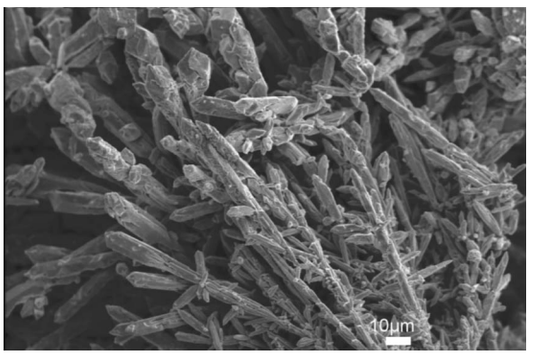

Figure 7. SEM picture of deposit obtained at 0.1 A cm^{-2} and 3500 rpm from the 0.019 M Fe solution. Current efficiency >70%, average theoretical thickness 116 µm.

the solution was very similar to the previous dissolution experiment. Iron-dissolved species, however, are not very stable, as revealed by the precipitation of red-brown compounds at the air/electrolyte interface after a few hours.

The current efficiency of the deposition was more than 70%, although hydrogen evolution could be expected during most of the test. The importance of this side reaction might be reduced because of a higher overpotential, possibly due to the inhibition properties of the dissolved iron species. Moreover, the first stage of cathodic polarization (10^4 s) in alkaline media is detrimental to hydrogen evolution, because hydrogen atoms adsorb on the electrode substrate and then create a higher overvoltage.[16] The deposit of appreciable thickness consisted mainly of dendrites and exhibited little compactness (Fig. 7). The oxygen content of the deposit was checked by EDS analysis, which revealed more than 98% Fe.

Voltammetric investigation.— The solution produced by anodic dissolution of iron and containing 0.019 M Fe species was used for this part of the investigation. As was done with hematite, the effect of cathodic potential limit on cyclic voltammetry was tested and is presented in Fig. 8.

A first reaction occurred between −900 and −1250 mV/SHE, where a well-defined current plateau (C1) near 0.01 A cm^{-2} was observed. The corresponding anodic plateau current (A1) was of the order of 0.001 A cm^{-2}, revealing the higher concentration of the

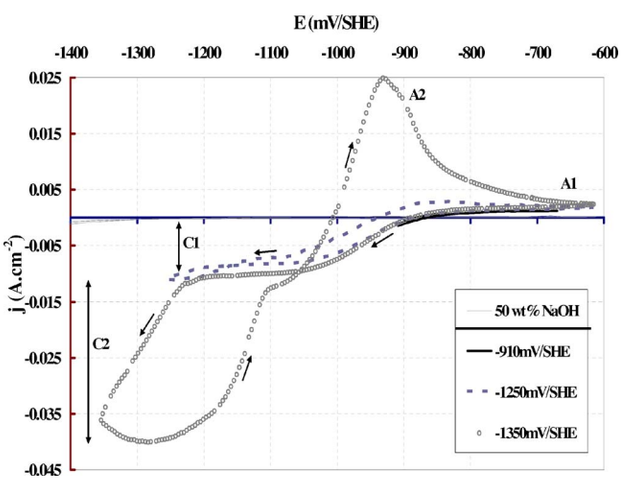

Figure 8. (Color online) Voltammograms obtained in 0.019 M dissolved Fe (18 M NaOH) solutions at 10 mV s^{-1} and 2500 rpm. Potentials given are the limits of the cathode scans while the anodic potential limit was kept at −630 mV/SHE. T = 110°C.

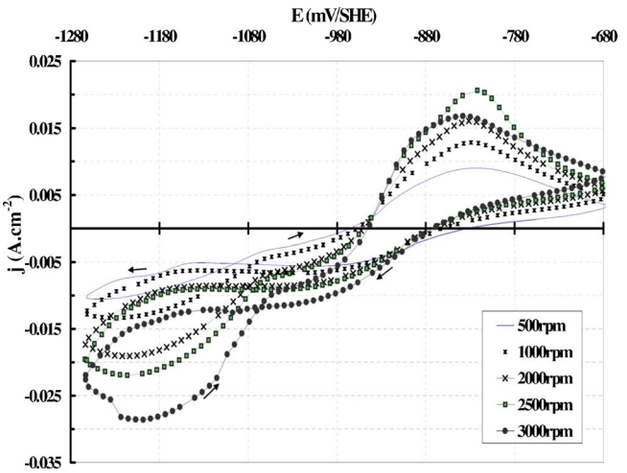

Figure 9. (Color online) Effect of the rotating speed on voltammograms recorded at 20 mV s^{-1} in 0.019 M Fe alkaline solutions. T = 110°C.

oxidized species in comparison to the reduced form produced by this first reaction. At more cathodic potentials, a second reaction occurred (C2 signal) which could be attributed to metal deposition, as indicated by the loop observed on the reverse scan. As explained in Ref. 19 or 20, this loop corresponds to the nucleation step on the forward scan, which limits iron deposition on the graphite electrode surface. This limitation is overstepped on the backward part of the curve, resulting in an increased current. The anodic peak (A2) appearing at −950 mV/SHE indicates the reversibility of this second reaction. The calculation of the net charge gives 0.95 C for the C2 loop (from −1090 to −1350 mV/SHE and backward) and 0.26 C for the anodic peak (from −1000 to −660 mV/SHE). Subtracting the charge corresponding to the C1 plateau current passing during the loop (0.41 C) from the overall C2 charge leads to an A2/(C2-C1) ratio of 0.48. This ratio corresponds to the faradaic efficiency of iron deposition, the complement at 52% being for hydrogen evolution.

The effect of the rotating speed on the voltammetric response of the system is presented in Fig. 9: both current plateau C1 and C2 signals are mass-transfer controlled. The corresponding Levich plot is given in Fig. 10 for the two cathodic reactions: the C1 current was taken as the current measured in the forward scan at ca. −1100 mV/SHE, and the C2 was also taken from the forward scan

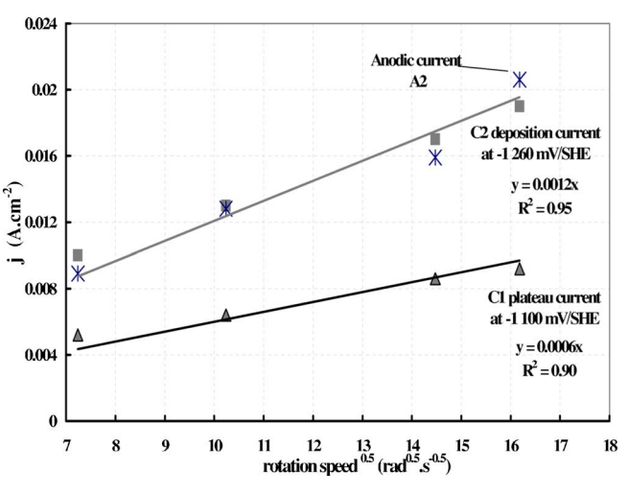

Figure 10. (Color online) Levich plots for the two cathodic reactions under study (triangles for C1 and squares for C2) and the anodic peak (cross for A2).

Table II. Chronoamperometry results for Fe deposition from the 0.019 M iron NaOH solution obtained by iron anode dissolution. Rotation rate = 3500 rpm.

Imposed potential (mV/SHE)	Average current density (mA cm^{-2})	Faradaic yield ($2e^-$ based, %)
−1090	7	37
−1160	16	48
−1230	23	67
−1290	29	53
−1330	38	50

at −1260 mV/SHE. The control by the mass-transfer rate also appeared in the anodic part of the *E-j* curves as shown in Fig. 10. The C2-over-C1 current ratio was observed to be independent of the rotating speed and was close to 2.

Chronoamperometric experiments were conducted at 3500 rpm with various cathode potentials for time periods ranging from 80 to 140 s. As shown in Table II, iron was deposited with good current efficiency (based on a two-electron requirement) in the potential range considered.

Discussion

Reactions of ferric ions in equilibrium with hematite.— As seen in Fig. 1, a very small current can be obtained for the reduction of the alkaline electrolyte saturated with dissolved hematite. Referring to thermodynamics and previously published results, the observed plateau C1 can be attributed to the reduction of ferric ions into ferrous species and the limiting current density is expressed by the Levich law

$$j_{\text{lim}} = 0.62nFCD^{2/3}\nu^{-1/6}\omega^{1/2} \quad [11]$$

The kinematic viscosity of the solution ν was estimated at 1.5×10^{-6} m^2 s^{-1} from the density and the viscosity of the solution (1595 kg m^{-3} and 2.4×10^{-3} Pa s for a 50 wt % NaOH solution at 110°C).[21] The concentration was taken at 2.64×10^{-3} M of ferric ion as determined by ICP and a single-electron exchange was assumed. Equation 11 led to

$$j_{\text{lim}} = 1.47 \times 10^6 \times D^{2/3}\omega^{0.5} \quad [12]$$

The diffusion component of the current for reduction of Fe(III) species was estimated from the Koutecky–Levich plot of the first-wave current (Fig. 3) at 1.9×10^{-9} m^2 s^{-1}. This value is consistent with the value estimated from the data in Ref. 12 at 7×10^{-10} m^2 s^{-1} for both Fe(II) and Fe(III) ions in KOH 10 M at 25°C (Fig. 5 in Ref. 12).

The reverse reaction is also observed in Fig. 3, where the oxidation current (peak A1) of the ferrous species formed during the previous scan is lower than that measured for the direct scan. Fe(II) leaves the vicinity of the cathode by convection and its concentration at the electrode during the anodic scan could be reduced as a consequence. As a matter of fact, high rotation speeds were observed to be detrimental to this anodic current. The height of the second peak A2 increases with rotation speed and, considering its potential, the A2 peak is linked to iron oxidation. The variation of the peak height with mass-transfer rate is then highly dependent on the amount of iron deposited and cannot be quantified rigorously.

Considering the cathodic reactions, the measured potentials are very close to those predicted by thermodynamic analysis: the reduction of ferric ions is possible and can be carried out at moderate overpotentials. The occurrence of a ferric/ferrous species equilibrium in the electrolyte saturated with hematite can be established as follows

$$Fe(OH)_4^- + e^- = Fe(OH)_3^- + OH^- \quad [13]$$

with an equilibrium potential at −870 mV/SHE and a limiting current density (plateau C1) of the order of 1 mA/cm^2.

Iron is then deposited through Fe(II) reduction

$$Fe(OH)_3^- + 2e^- = Fe + 3\ OH^- \quad [14]$$

but its formation is in severe competition with hydrogen evolution. Due to the low amount of soluble species, the deposition potential at equilibrium is close to −1220 mV/SHE in the conditions considered. Besides, the deposition current density at −1250 mV/SHE was estimated at 0.5 mA cm^{-2} from the overall current density (Table I), after subtracting the hydrogen current estimated from the deposition current efficiency.

Reactions of dissolved species at high concentration.— High concentrations of dissolved iron (near 0.02 M) can be obtained, e.g., by galvanic coupling between iron and a more noble material in alkaline media. Anodic dissolution is rather slow, as seen in Fig. 7, but iron deposition from dissolved species occurs with a high efficiency. Corrosion of the anode leads to ferrous ions, as revealed by the color of the solution, but the oxidation to ferric species cannot be discarded as explained below.

At 1000 rpm, the cathodic current for the C1 plateau (Fig. 8) is six times higher than in the case of hematite dissolution (Fig. 1). Levich's plot (Fig. 8) yields a diffusion coefficient of 4.2×10^{-10} m^2 s^{-1} for ferric ions. The current for the anodic reverse reaction A1 confirms the low amount of ferrous ions. The current density values at 0.01 A cm^{-2} (C1) and 0.001 A cm^{-2} (A1), together with the measured equilibrium potential near −850 mV/SHE, imply that the Fe(III)/Fe(II) ratio is around 10.

The deposition reaction (Eq. 5) is shown by the hysteresis appearing on the reverse scan in Fig. 8 and 9 and was confirmed by chronoamperometry. The hysteresis becomes more significant with higher mass-transfer rates of the reactive species. The Levich plot of the current related to Reaction 5 presented in Fig. 10 gives a diffusion coefficient of 4.2×10^{-10} m^2 s^{-1}, assuming two electrons exchanged and considering ferrous ion concentration at 0.019 M. This calculation can be justified by the mass balance on iron for the case of two consecutive electrochemical reductions (cf. Appendix), considering that the two current waves are separated by 150 mV potential difference. Due to the large concentration of reactants, the potential remains in a range where hydrogen evolution is less important; high deposition current yield can then be expected. Moreover, high rotation rates restrict the adherence of hydrogen bubbles near the disk electrode edge which could hinder deposition.

Overall process: dissolution and deposition of iron in alkaline media.— Electrodeposition conducted with an electrolyte saturated with ferric ions produced by hematite dissolution was shown to lead to metal iron, however, with a very low efficiency, whereas the deposition conducted in the presence of suspended ore particles can be carried out with high yields at 0.1 A cm^{-2}. Metal iron can also be obtained with high production rates from more concentrated solutions prepared by dissolving iron anodes, as shown in this paper. The exact mechanism of the dissolution process of iron in alkaline media is still under discussion in the electrochemical community, but published results[15,22] mention the conversion of iron into magnetite on the metal. The dissolution of magnetite can thus generate both ferric and ferrous ions. For the case under study in the previous section, the electrolyte resulting from iron anode dissolution contains a large concentration of dissolved species, with 10 times more ferric than ferrous ions. In the overall reduction mechanism of hematite to iron metal, the direct reduction of ions produced by the dissolution of iron oxide particles cannot be considered as the only occurring reaction. The contribution of ionic species, though, can be considered by dissolution of an intermediate magnetite oxide that still needs to be identified. The characterization of magnetite dissolution and its reduction in alkaline media is then a key issue to identify the reaction pathway, in particular, to establish whether ions or solid phase are involved in the deposition. This would allow a complete mechanism to be suggested, with the various steps for conversion of oxide particles to iron.

Conclusion

The electrochemical study of an iron oxide saturated solution has shown that hematite iron oxide is in equilibrium with ferric ion species at 2.6×10^{-3} M in 18 M NaOH at 110°C. A diffusion coefficient of the order of 1.9×10^{-9} m^2 s^{-1} was determined for this ion by studying the Fe(III)/Fe(II) equilibrium. Deposition of the formed ferrous species is possible with low overpotential in such low concentrated media. The efficiency of the deposition is far higher, with higher concentrations of iron species in the solution. Such conditions can be obtained by dissolving an iron metal source by galvanic coupling with a nobler material. The link between the poorly soluble hematite iron(III) oxide and this large amount of dissolved species obtained in a transient state should help us, in the future, to improve the understanding of the overall reduction mechanism of iron ore in alkaline media.

Acknowledgments

The authors are grateful to the EU 6th Framework Program for its financial support of the ULCOS project.

Arcelor Research assisted in meeting the publication costs of this article.

Appendix

Calculation of Limiting Current Density in the Case of Two Consecutive Electrochemical Reactions

Considering the two consecutive reactions

$$A + n_A e^- \rightarrow B \text{ at } E_A \text{ potential} \quad [A\text{-}1]$$

and

$$B + n_B e^- \rightarrow C \text{ at } E_B \ll E_A \text{ potential} \quad [A\text{-}2]$$

The current density for Reaction A-1 in limitation by mass transfer of A is

$$j_A = - n_A F k_L C_A^b \quad [A\text{-}3]$$

where C_A^b is the concentration of A in the bulk of the electrolyte and k_L is the mass-transfer coefficient from the bulk of the solution to the electrode.

The current density for Reaction A-2 is

$$j_B = - n_B F K_R^B C_B^s$$

$$\text{with } K_R^B = k_B^\circ e^{-\beta_B E} \quad [A\text{-}4]$$

where k_B° is a kinetic constant for the reaction, $\beta_B = \alpha_R^B n_B^{lim}/RT$ where α_R^B is the symmetry factor, n_B^{lim} is the number of electrons involved in the limiting step, E is the electrode potential, and C_B^s is the concentration of B at the electrode surface.

The mass balance on B created by Eq. A-1, arriving by mass transfer from the bulk and consumed by Eq. A-2 in steady state at the electrode, gives

$$k_L C_A^b + k_L (C_B^b - C_B^s) = K_R^B C_B^s$$

The concentration at the electrode for B is then, considering sufficiently high value of the potential E

$$C_B^s \approx \frac{k_L}{K_R^B}(C_B^b + C_A^b)$$

and Eq. A-4 becomes

$$j_B = - n_B F k_L (C_A^b + C_B^b) \quad [A\text{-}5]$$

Such an equation predicts that the ratio between j_A (Eq. A-3) and j_B (Eq. A-5) is directly equal to the exchanged electron ratio for the two reactions, providing concentration of A is higher than B within the bulk of the electrolyte.

References

1. S. J. Lloyd, *Trans. Am. Electrochem. Soc.*, **55**, 305 (1929).
2. J. A. M. Leduc, R. E. Loftfield, and L. E. Vaaler, *J. Electrochem. Soc.*, **106**, 659 (1959).
3. D. E. Hall, *J. Electrochem. Soc.*, **128**, 740 (1981).
4. C. L. Mantell, *Industrial Electrochemistry*, McGraw-Hill, New York (1931).
5. A. Calusaru, *Electrodeposition of Metal Powders*, Elsevier, Amsterdam (1979).
6. G. Picard, D. Oster, and B. Tremillon, *J. Chem. Res., Synop.*, 252 (1980).
7. I. I. Diakonov, J. Schott, F. Martin, J. Harrichourry, and J. Escalier, *Geochim. Cosmochim. Acta*, **63**, 2247 (1999).
8. B. Beverskog and I. Puigdomenech, *Corros. Sci.*, **38**, 2121 (1996).
9. J. Balej, *Collect. Czech. Chem. Commun.*, **61**, 1549 (1996).
10. B. Andersson and L. Ojefors, *J. Electrochem. Soc.*, **123**, 824 (1976).
11. H. H. Le and E. Ghali, *J. Appl. Electrochem.*, **23**, 72 (1993).
12. R. D. Armstrong and I. Baurhoo, *J. Electroanal. Chem.*, **40**, 325 (1972).
13. F. Beck, R. Kaus, and M. Oberst, *Electrochim. Acta*, **30**, 173 (1985).
14. K. Bouzek, I. Rousar, H. Bergmann, and K. Hertwig, *J. Electroanal. Chem.*, **425**,

125 (1997).
15. S. Giddey, B. Cherry, F. Lawson, and M. Forsyth, *Corros. Sci.*, **43**, 1497 (2001).
16. L. Brossard and J. Y. Huot, *J. Appl. Electrochem.*, **21**, 508 (1991).
17. R. Scholder, *Angew. Chem.*, **49**, 255 (1936).
18. R. G. Doisneau and B. Tremillon, *Bull. Soc. Chim. Fr.*, **9–10**, 1419 (1976).
19. P. J. Sonneveld, W. Visscher, and E. Barendrecht, *Electrochim. Acta*, **37**, 1199 (1992).
20. M. J. Lain and P. Pletcher, *Electrochim. Acta*, **32**, 99 (1987).
21. M. A. Klochko and M. M. Godneva, *Russ. J. Inorg. Chem.*, **4**, 964 (1959).
22. S. E. Ziemniak, M. E. Jones, and K. E. S. Combs, *J. Solution Chem.*, **24**, 837 (1995).